Available online at www.sciencedirect.com
ScienceDirect
Journal of Power Sources 173 (2007) 743–747
JOURNAL OF POWER SOURCES
www.elsevier.com/locate/jpowsour

Short communication

Nanocrystallization as a method of improvement of electrical properties and thermal stability of V_2O_5-rich glasses

J.E. Garbarczyk *, P. Jozwiak, M. Wasiucionek, J.L. Nowinski

Faculty of Physics, Warsaw University of Technology, Koszykowa 75, 00-662 Warsaw, Poland

Available online 24 May 2007

Abstract

Vanadia-rich glasses of the Li_2O–V_2O_5–P_2O_5 system (predominantly electronic conductors) and V_2O_5–P_2O_5 one (purely electronic conductors) – potential cathode materials for lithium ion batteries – were investigated by impedance spectroscopy (IS), differential scanning calorimetry (DSC), X-ray diffractometry (XRD) and scanning electron microscopy (SEM). It was shown that the electrical conductivity of the original glasses of both systems can be considerably enhanced by appropriate annealing at temperatures close to crystallization temperature T_c. Moreover, the resulting materials are thermally stable up to ca. 350 °C, i.e., some 100 °C higher than the glass transition of the initial glasses. Increase in conductivity arises from the modification of the microstructure. It was found out by XRD and SEM studies, that by appropriate heat treatment glasses of both systems can be turned into nanomaterials consisting of crystalline grains of V_2O_5 of ca. 30 nm average size embedded in the glassy matrix. It was postulated that the major role in the conductivity enhancement of these nanomaterials is played by the developed interfacial regions between crystalline and amorphous phases, in which the concentration of V^{4+}–V^{5+} pairs responsible for electron hopping, is higher than inside the glassy matrix. The annealing at temperatures exceeding T_c leads to massive crystallization and to a conductivity drop.

Keywords: Nanocrystallization; Nanomaterials; Vanadate–phosphate glasses; Cathode materials

1. Introduction

Vanadium oxides and phosphates belong, together with lithium-manganese-oxide spinels, lithium nickel-cobalt oxides and olivines, to the most studied materials for cathodes in lithium-ion rechargeable batteries [1–4]. Majority of these materials are polycrystalline. Substantially less is known about lithium–vanadate glasses [5] or glassy-crystalline nanomaterials suitable for battery applications. It was shown [6], that glasses of the Li_2O–V_2O_5–P_2O_5 system are mixed electronic–ionic conductors in which the proportions of the electronic-to-ionic components of the conductivity depend on the ratio r between contents of a glass modifier (Li_2O) and glass formers ($V_2O_5 + P_2O_5$): $r = [Li_2O]/([V_2O_5] + [P_2O_5])$. Use of these glasses as potential cathode materials for lithium batteries requires that the conduction is mainly electronic. This occurs in V_2O_5-rich glasses of the Li_2O–V_2O_5–P_2O_5 or V_2O_5–P_2O_5 systems. An additional increase in conductivity of these glasses can be achieved after their nanocrystallization, induced by an appropriate annealing process [7,8]. The aim of this paper is a comparison of temperature dependences of conductivity, microstructure, thermal events and characteristics of crystallization phenomena in the case of vanadia-rich systems containing lithium (Li_2O–V_2O_5–P_2O_5) and lithium-free (V_2O_5–P_2O_5).

2. Experimental

Two series of vanadate–phosphate glasses were prepared—one containing lithium and one lithium-free. Their compositions were described by respective formulas: (i) $xLi_2O\cdot(100-2x)V_2O_5\cdot xP_2O_5$, for $15 \le x \le 45$ and (ii) $xV_2O_5\cdot(100-x)P_2O_5$, for $60 \le x \le 90$. Samples were prepared from pre-dried chemicals: V_2O_5 (ABCR, 99.9%), $NH_4H_2PO_4$ (POCh, 99.9%) and $LiNO_3$ (Aldrich, 99.9%), by a standard melt-quenching technique described in ref. [8]. X-ray diffractometry (XRD) measurements were carried out at room temperature using a Philips X'Pert Pro diffractometer. They confirmed the absence of crystalline phases in as-received samples. Differential scanning calorimetry (DSC) scans were run in air on a Perkin-Elmer DSC Pyris 1 instrument in the temperature range 20–550 °C at the 20 K min^{-1} scan rate. They provided information on

* Corresponding author.
E-mail address: garbar@if.pw.edu.pl (J.E. Garbarczyk).

0378-7753/$ – see front matter © 2007 Published by Elsevier B.V.
doi:10.1016/j.jpowsour.2007.05.069

the temperatures of glass transition T_g and crystallization T_c. Electrical properties were studied by impedance spectroscopy in the 50 mHz to 10 MHz frequency range. The experimental system for impedance spectroscopy measurements included a Solartron 1260 Gain Phase/Impedance Analyzer, a furnace and a system of temperature control and stabilization. Sequences of heating/cooling cycles from room temperature to characteristic temperatures (close to T_g and T_c determined from the DSC), were carried out in order to reveal how the formation of crystallites correlates with changes of the electronic conductivity. The conductivity measurements were done in air. XRD patterns of samples annealed at given temperatures provided information on the presence of crystalline phases, their identification and average grain size. Microstructure of the samples under study and in particular the crystalline grains formed as a result of nanocrystallization or massive crystallization, were observed by Field Emission Scanning Electron Microscopy (FE-SEM) using a LEO 1530 set-up.

3. Results and discussion

3.1. Glass of composition $15Li_2O{\cdot}70V_2O_5{\cdot}15P_2O_5$

Impedance spectra of glasses of this composition (but also those of the $90V_2O_5{\cdot}10P_2O_5$ glass) consist of a single arc, which at low frequencies reaches the Re z-axis. No low-frequency spur is observed. This shape is characteristic for predominantly or purely electronic conductors, whose charge carriers are not blocked at the electrodes (here sputtered gold). This observation agrees with the expectation that glasses with high content of vanadium and low content of Li_2O like the glass of composition $15Li_2O{\cdot}70V_2O_5{\cdot}15P_2O_5$ are predominantly electronic conductors (charge transport occurs via electron hopping between neighboring aliovalent V^{4+} and V^{5+} centres). Impedance spectra of nanomaterials described below consisted of a single distorted arc. DSC trace of a glass of composition $15Li_2O{\cdot}70V_2O_5{\cdot}15P_2O_5$ (upper part of Fig. 1) reveals a baseline shift characteristic for the glass transition at $T_g = 260\,^{\circ}C$ and an exothermic peak of crystallization at $T_c = 311\,^{\circ}C$. Fig. 1 also shows the temperature dependence of conductivity during a cycle consisting of heating up to 311 °C (label 1 in Fig. 1), annealing at that temperature for 7 h and cooling down to room temperature (label 2 in Fig. 1). Up to the glass transition T_g this dependence follows the Arrhenius formula with the activation energy equal to 0.41 eV below 140 °C. This value is close to those reported in literature for other V_2O_5-rich glasses, e.g., ref. [9]. Above 140 °C the slope slightly increases. This change of the activation energy in the 140–260 °C range can result from the gradual variation of the proportion between electronic and ionic components of the total conductivity of this mixed conductor. Such a change is feasible even in a very simple situation when both types of charge carriers: electrons and Li^+ ions move independently from each other, and activation energy values characteristic for their transport are different [10].

At about 260 °C, i.e., at the glass transition temperature T_g, the conductivity undergoes a fast non-Arrhenian increase, which extends up to $T_c \approx 311\,^{\circ}C$. It is interesting to note that the temperature dependence of the conductivity in this range can be satisfactorily fitted using the Vogel–Tammann–Fulcher (VTF) formula. This observation was already discussed in our earlier paper [7]. Heating was stopped at 311 °C and the sample was annealed at that temperature (equal to T_c from DSC) for 7 h in order to complete crystallization processes. No changes in conductivity were observed during the annealing. This means that the kinetics of the crystallization process at T_c is so fast that it completes during the period of temperature stabilization and the first impedance measurement at that temperature. On cooling the temperature dependence of conductivity followed the Arrhenius formula with the single activation energy down to room temperature. The value of the activation energy (0.27 eV) was much lower than that observed during heating (0.41 eV). Another advantageous effect of the annealing was a considerable conductivity increase—conductivity values at 200 °C and at room temperature were by one and two orders of magnitude, respectively, higher on cooling than on heating.

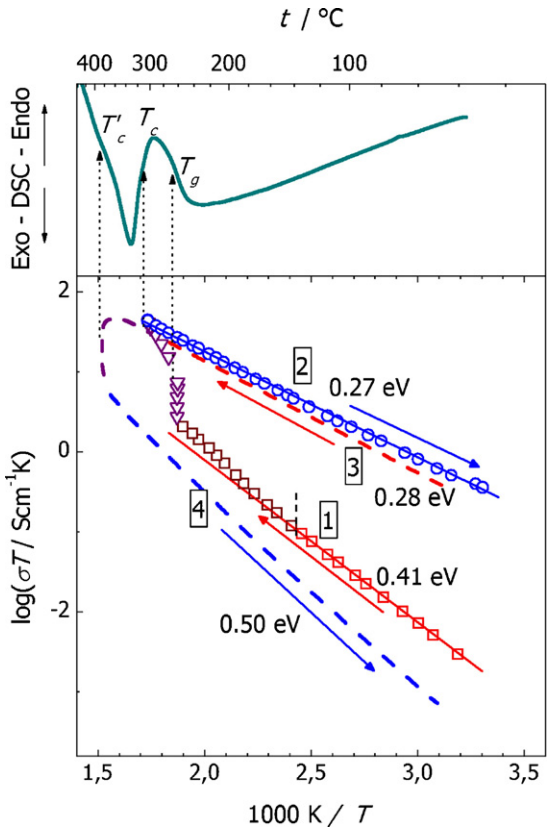

Fig. 1. Thermal history of a glass of composition $15Li_2O{\cdot}70V_2O_5{\cdot}15P_2O_5$ during nanocrystallization by annealing. Upper part—DSC curve. Lower part—temperature dependences of electrical conductivity. Numbers in boxes denote consecutive heating and cooling stages. For clarity, the experimental points in the runs 3 and 4 are omitted. Further details are in the text.

In order to check if this enhanced conductivity is stable and reproducible, we performed a series of conductivity measurements during the second heating–cooling cycle (denoted by labels 3 and 4 in Fig. 1). On heating, the conductivity closely followed the Arrhenian dependence from cooling stage in the first cycle up to temperature 360 °C, exceeding by 50 °C the temperature of the crystallization and by 100 °C the glass tran-

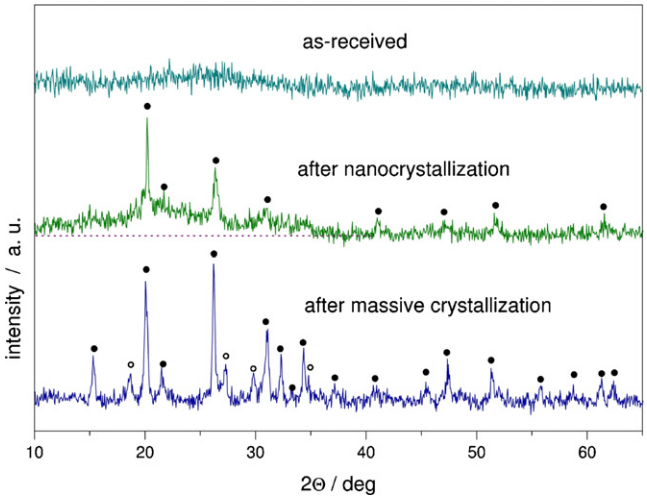

Fig. 2. XRD patterns of the sample of composition $15Li_2O{\cdot}70V_2O_5{\cdot}15P_2O_5$: as-received (top); after annealing at $T_c = 311\,^{\circ}C$ for 7 h (middle); after additional annealing at 398 °C for 5 h (bottom). Peaks corresponding to crystalline V_2O_5 are marked by filled circles. Open circles denote unidentified crystalline phase.

sition temperature (Fig. 1). It is an indication that the material is thermally stable to temperature about 100 °C higher than the stability limit of the initial glass (260 °C). Above 360 °C the conductivity begins to deviate from Arrhenius-like behavior. At 400 °C it started to decrease. After a drop of conductivity by more than one order of magnitude observed at 400 °C, the sample was cooled down to room temperature (stage 4 in Fig. 1). The conductivity changed with temperature according to Arrhenius formula. Activation energy was 0.50 eV in the whole 20–400 °C temperature range.

All above listed effects were ascribed to structural changes occurring during heat-treatment: initially heated glasses, and additionally annealed glass-crystalline materials. A series of XRD structural studies were done on samples at different stages of the crystallization process. The diffraction patterns are shown in Fig. 2. In the case of as-received materials (upper pattern), there is only a wide halo observed with no indication of diffraction peaks. This confirms the amorphous state of initial glasses. A pattern shown in the middle part of Fig. 2 was collected for a sample after its annealing at crystallization temperature $T_c = 311\,^{\circ}C$. There are a number of crystalline peaks superimposed on a wide halo pointing to the presence of amorphous phase. Such a structure of the XRD pattern clearly shows that the annealing at temperature T_c only starts to produce small crystallites in the glass matrix. The crystalline phase was identified as orthorhombic V_2O_5. The average size of crystallites was estimated from the width of diffraction peaks using the Scherrer formula, to ca. 30 nm. The second annealing, this time at temperature close to 400 °C, considerably exceeding temperature T_c and slightly exceeding temperature T_c' (Fig. 1), leads to massive crystallization (Fig. 2). After this stage, the XRD pattern does not contain a halo and peaks corresponding to V_2O_5 are much stronger and sharper. Additionally, there are some new peaks corresponding to the phase which we have not identified yet. The estimate of average grain size at this stage is close to 100 nm. Microscopic observations revealed, however, also the presence of larger grains of V_2O_5 (up to 1 μm). It seems that the large size of these grains and their dense packing reduces space required for long-range ionic conduction. Therefore, the temperature dependence of the electrical conductivity in the stage 4 in Fig. 1 we interpret as due to the electronic component alone.

3.2. Glass of composition $90V_2O_5{\cdot}10P_2O_5$

A primary difference between the $90V_2O_5{\cdot}10P_2O_5$ and $15Li_2O{\cdot}70V_2O_5{\cdot}15P_2O_5$ glasses is the absence of the Li_2O in the former case. This absence causes that the $90V_2O_5{\cdot}10P_2O_5$ glass cannot conduct Li^+ ions that makes the interpretation of the conductivity results more clear.

In case of the $90V_2O_5{\cdot}10P_2O_5$ glass several modifications, in comparison with the $15Li_2O{\cdot}70V_2O_5{\cdot}15P_2O_5$ composition were introduced concerning the sequence of conductivity measurements.

Firstly, a cycle was added consisting of a heating run up to glass transition temperature and a cooling down to room temperature. The aim of this cycle was to check whether the sample undergoes any conductivity changes being in purely amorphous state. Secondly, the annealing at the temperature close to crystallization temperature, which in the case of the glass $15Li_2O{\cdot}70V_2O_5{\cdot}15P_2O_5$ lasted for 7 h, now was reduced to the time needed for temperature stabilization and an impedance measurement only (ca. 0.5 h). Moreover, for the glasses $90V_2O_5{\cdot}10P_2O_5$ a series of SEM pictures were taken which had helped to evaluate the effect of the microstructure on the conduction process.

From the DSC trace of this glass (upper part of Fig. 3) one can find values of glass transition temperature and crystallization temperature. These values are similar to those of the $15Li_2O{\cdot}70V_2O_5{\cdot}15P_2O_5$ glass. The glass transition temperature T_g is slightly lower (255 °C versus 260 °C for the $15Li_2O{\cdot}70V_2O_5{\cdot}15P_2O_5$ glass) and the crystallization temperature T_c slightly higher (326 °C versus 311 °C, respectively). The temperature dependence of conductivity in the first cycle up to T_g follows the Arrhenius formula with a single activation energy of 0.37 eV on heating. On cooling the conductivity values are the same as on heating within a limit of an experimental error (Fig. 3, middle part). If the sample is heated to higher temperature, one can observe a non-Arrhenian increase of conductivity in the temperature range between T_g and T_c. On cooling the conductivity changes according to the Arrhenius formula with an activation energy of 0.28 eV, considerably lower than on heating (0.36 eV) and equal, within a limit of experimental error, to activation energy for nanostructural sample of composition $15Li_2O{\cdot}70V_2O_5{\cdot}15P_2O_5$. Moreover, conductivity values on cooling run are systematically higher than those found on heating. At 100 °C this difference is close to one order of magnitude. This means that also for this lithia-free glass the annealing at temperature close to T_c leads to the conductivity enhancement and to an increase in the upper temperature limit of thermal stability of the material.

SEM picture of the sample $90V_2O_5{\cdot}10P_2O_5$ heated up to 340 °C, near the crystallization temperature, shows the presence of many nanocrystallites (average size of ca. 30 nm) mostly cov-

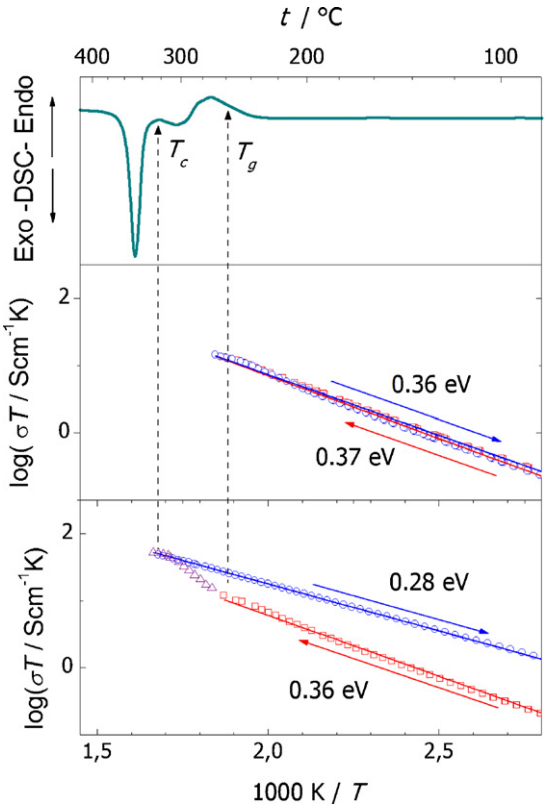

Fig. 3. Temperature dependence of conductivity of the glass $90V_2O_5{\cdot}10P_2O_5$ on heating (◯) up to ca. 270 °C ≈ T_g and cooling (□) runs (middle part); analogous dependence for a glass heated up to ca. 340 °C ≈ T_c (□ and △) and cooled down (◯) (bottom part). Solid lines denote best fit to experimental data. A corresponding DSC trace is shown in the upper part of figure.

ered by a thin layer of another phase (Fig. 4). A zoomed view of a fragment of the microstructure is shown in the inset in Fig. 4. Besides nanocrystallites one can see also some remnant glassy phase. Upon heating to much higher temperature (540 °C) a massive crystallization occurs and the microstructure changes considerably. Fig. 5 shows the presence of two types of crys-

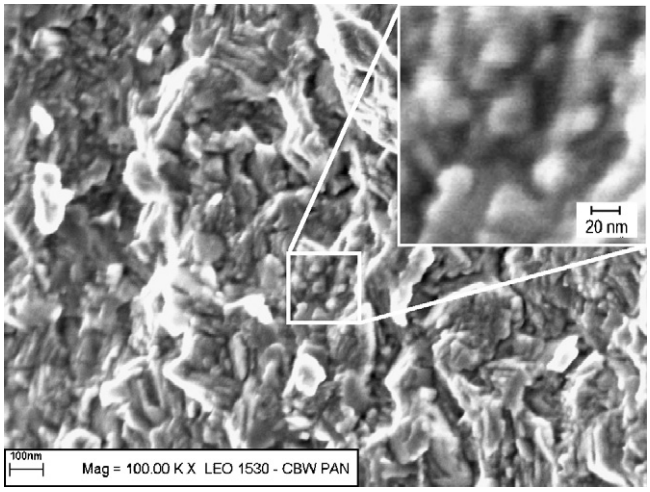

Fig. 4. SEM micrograph of a sample $90V_2O_5{\cdot}10P_2O_5$ after being heated up to 340 °C (i.e., close to T_c). A zoomed fragment of the picture with several nanocrystallites of V_2O_5 (average size ca. 30 nm) is visible on the right.

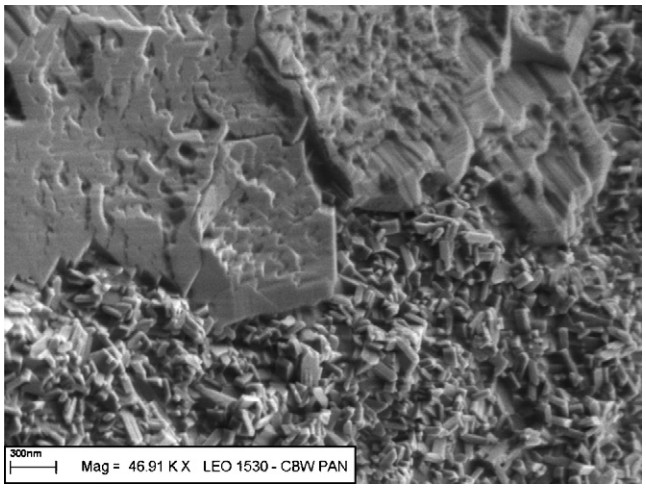

Fig. 5. SEM micrograph of a sample $90V_2O_5{\cdot}10P_2O_5$ after being heated up to 540 °C. There are many medium-size (100–300 nm) and large (about 1 μm) crystallites of V_2O_5. In the upper left part of Fig. 1 can see a region consisting of partly joined crystallites.

tallites: medium size (100–300 nm) and large grains (order of 1 μm). Similarly as in the case of the $15Li_2O{\cdot}70V_2O_5{\cdot}15P_2O_5$ samples, the crystalline phase was identified by XRD as the orthorhombic V_2O_5. The analysis of another SEM picture presenting only medium size grains evidently shows the presence of orthorhombic V_2O_5 crystallites of 100–300 nm size (Fig. 6).

The effects of the annealing at different temperatures on the conductivity and the microstructure show that the conduction process is closely correlated with the microstructure. To our knowledge there is no established theoretical model for conduction in glassy-crystalline nanomaterials exhibiting electronic conduction. Therefore, the proposed below interpretation of these correlations is based on the Mott model of conduction in vanadia-rich glasses, where the dominant process consists of the electron jumps between aliovalent V^{4+}–V^{5+} hopping centers via small polaron [11]. Some justification of such approach is an Arrhenian behavior of conductivity in nanomaterials under study. According to the Mott model, for $T > \theta/2$ (half of the

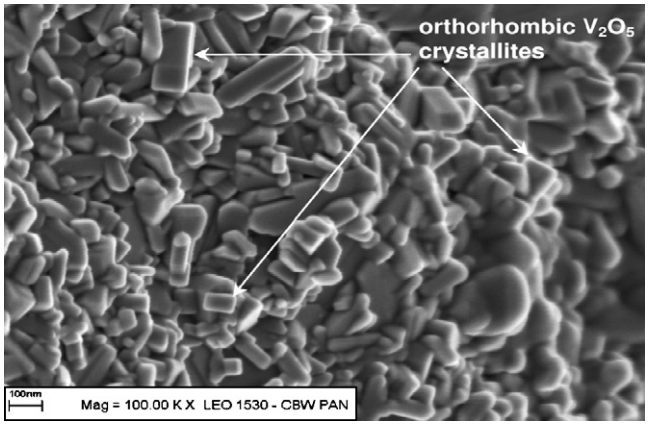

Fig. 6. SEM micrograph of the another part of a sample $90V_2O_5{\cdot}10P_2O_5$, heated up to 540 °C, containing only medium-size (100–300 nm) grains. Individual orthorhombic crystallites of V_2O_5 are visible.

Debye temperature) the conductivity is expressed by a formula:

$$\sigma = \frac{e^2 c(1-c)}{kRT} \nu_e \, e^{-2\alpha R} \, e^{-E_e/kT} = \sigma_{e0} \, e^{-E_e/kT} \quad (1)$$

where R is the average distance between hopping centers, $\nu_e = \hbar/mR^2$, α the inverse localization length of the electron wave function, c the fraction of hopping sites occupied by electrons and E_e is the activation energy of electronic conduction. The theoretical expression for that energy includes a term $W = W_0(1 - r_p/R)$, where W_0 is constant and r_p denotes a radius of small polaron [11]. All above formulas indicate that electronic conductivity increases and activation energy decreases when the distance R between hopping centers decreases. In our case one can expect that due to nanocrystallization process the concentration of V^{4+}–V^{5+} pairs is higher near the surfaces of the newly formed crystallites than in the remaining glassy phase and inside the crystallites. It is widely known that many important characteristics of nanomaterials originate from the defective nature of the interfaces between crystalline and amorphous phases. Higher concentration of V^{4+}–V^{5+} pairs leads to smaller average distance between the hopping centers, and according to the Mott model it causes an increase in conductivity. The interface regions of higher than average conductivity form a kind of "easy conduction paths" for electrons. In the inset in Fig. 4 such conducting paths could be located along the visible nano-size crystallites. Similarly, as in the case of the $15Li_2O{\cdot}70V_2O_5{\cdot}15P_2O_5$ glass, massive crystallization caused by annealing at temperatures higher than T_c leads to a drop of the conductivity. This effect may be understood as a result of the partial blocking of electrons at the grain boundaries of the polycrystalline sample and the decrease of the easy conduction paths density.

4. Conclusions

The annealing of the V_2O_5-rich glasses to T_c leads to their nanocrystallization (V_2O_5 nanocrystallites ca. 30 nm embedded in a glassy matrix). The resulting nanomaterials exhibit much higher electronic conductivity (10^{-1} S cm^{-1} at 300 °C and 3×10^{-3} S cm^{-1} at room temperature) and much lower activation energy ($E = 0.27$ eV) than the initial glasses. Furthermore, they are stable up to ca. 350 °C, i.e., some 100 °C higher than T_g of the initial glasses. A conductivity enhancement can be attributed to (i) an increase of concentration of V^{4+}–V^{5+} pairs, and (ii) formation of defective, well-conductive regions along the glass-crystallites interfaces. Further annealing of the samples up to 400–500 °C leads to their massive crystallization and decrease of the electronic conductivity.

Acknowledgement

Authors are grateful to Dr. S.Gierlotka from the Institute of High Pressure Physics, Polish Academy of Sciences, for his help in carrying out SEM investigations.

References

[1] M.S. Whittingham, Chem. Rev. 104 (2004) 4271–4301.
[2] C.P. Grey, N. Dupré, Chem. Rev. 104 (2004) 4493–4512.
[3] A.K. Pahdi, K.S. Najundaswamy, J.B. Goodenough, J. Electrochem. Soc. 144 (1997) 1188–1194.
[4] M. Wakihara, Mater. Sci. Eng. R33 (2001) 109–134.
[5] J.L. Souquet, A. Kone, M. Levy, in: W.J.R. Akridge, M. Balkanski (Eds.), Solid State Microbatteries, vol. 217, NATO ASI Series B: Phys., 1990, pp. 301–322.
[6] P. Jozwiak, J.E. Garbarczyk, Solid State Ionics 175 (2005) 2163–2166.
[7] J.E. Garbarczyk, P. Jozwiak, M. Wasiucionek, J.L. Nowinski, Solid State Ionics 175 (2004) 691–694.
[8] J.E. Garbarczyk, P. Jozwiak, M. Wasiucionek, J.L. Nowinski, Solid State Ionics 177 (2006) 2585–2588.
[9] S. Sen, A. Ghosh, Phys. Rev B 60 (1999) 15143–15149.
[10] P. Jozwiak, J.E. Garbarczyk, M. Wasiucionek, Mater. Sci. 24 (2006) 147–153.
[11] I.G. Austin, N.F. Mott, Adv. Phys. 18 (1969) 41–102.